Proceedings of the Project Review, Geo-Mathematical Imaging Group (Purdue University, West Lafayette IN), Vol. 1 (2012) pp. 13-27.

TIME EXTENDED STRUCTURE TENSORS FOR MULTIPLE DIRECTIONALITY ESTIMATION

FREDRIK ANDERSSON*

Abstract. A novel method for extending structure tensors by using the one way wave equation is proposed. This allows for the detection of two intersecting waves in the two dimensional case. In three dimensions both two and three intersecting waves can be detected. Moreover, a method for directionality filtering using the estimated directions is proposed. This method also relies on a particular usage of the one way wave equation.

1. Introduction. Structure tensors have proven to be a useful tool for local orientation estimations in a large range of applications in image processing, including anisotropic diffusion [16, 18, 14], image regularization [3, 17] and image compression [8] to name a few. They were first introduced in [7] for edge and corner detection, and have ben widely used for that purpose [6, 9, 13, 19].

Structure tensors are formed by averaging the outer product of the gradient of an image, or a counterpart in higher dimensions. Without the average, this constructed tensor would clearly be of rank one. This is no longer the case when averaging is performed, but if the image has a locally dominant direction, one of the eigenvalues will be significantly larger than the other one (in two dimensions), and the eigenvector corresponding to that eigenvalue will align with the dominant direction.

While structure tensors provide a stable way of making directionality estimation of for instance edges or wavefronts, only one direction can be recovered in the standard setup. For the case of two intersecting edges — or two intersecting local waves with different directions — this approach fails. The eigenvectors do no longer align with the directions of the edges or waves (or, more generally the wave front set of the function). Hence, the standard approach of using structure tensors breaks down in the presence of intersecting edges or waves. For some data sets, in particular such associated with seismics, intersecting waves appear frequently and this restricts the usability of structure tensors as a directionality analysis tool.

A few different approaches have been suggest in the literature to address this problem. For instance, a two step procedure using directionality voting into bins was introduced in [1].

A generalization to the standard structure tensor is to use higher order outer products to form *higher order structure tensors*. Such discussed for instance in [12, 15, 14]. In [15] novel glyphs for higher-order structure tensors are introduced. Generalized eigendecompositions for multilinear algebra is used [10] instead of ordinary eigenvalue decomposition. A problem with this approach seems to be that the methods for generalized eigendecompositions for higher order structure tensors are rather computationally intense. The novel glyphs introduced [15] also seems harder to quantify and interpret than the eigenvectors of the standard second order structure tensor. An advantage, however, seems to be that the framework allows for many intersecting oscillations. The number of elements of an order l tensor in n dimensions has n^l tensor channels, but the number of independent channels are reduced to $\binom{n+l-1}{l}$ in the totally symmetric case. According to [15, Figure 3.2] it is enough to use fourth order ($l = 4$) structure tensors to distinguish two intersecting edges, but increased orders ($l = 10$ and $l = 50$ are reported) provide more accurate models.

In this paper a different approach is proposed. For the two-dimensional case, images are extended to three dimensions (space—time) by applying a one way wave equation with constant velocity to the original data. This have the advantage that purely oscillatory function in space will become purely oscillatory functions in the extended space–time domain. For the case where the function, or image, is (locally) a sum of two waves with different directions, the structure tensor computed in the extended domain will be of size 3×3, but of rank two. Although this seems promising it is easily seen that this is not sufficient for reconstructing the two directions. However, it is possible to make use of fact that the extension was made through the wave equation. This fact

*Centre for Mathematical Sciences, Lund University, Box 118, SE-22100 Lund Sweden, (fa@maths.lth.se).

restricts the set of possible 3×3 tensors enough to uniquely determine the directions of oscillation (a limit result).

The three dimensional case can be treated in a similar manner. The problem of recovering two directions follows immediately from the two-dimensional setup, and it is possible to construct a method where three intersecting waves can be recovered, although it requires a bit more work. In the two dimensional case, the recovery problem can be formulated in terms of a second eigenvalue problem (of size 2×2), using the values of the eigenvector corresponding to the smallest eigenvalue of the 3×3 tensor, as entries. For the recovery of three directions in the three dimensional case, it is necessary to use 5×5 tensors. Moreover, the three directions can be recovered by solving a system of two polynomials in two variables. The coefficients of these two polynomials are given in terms of the elements of the eigenvectors corresponding to the two smallest eigenvalues of the 5×5 tensor.

An advantage with this method is that all operations are comparatively cheap, and that estimates are easy grasp (simply directions in $\mathbb{R}^q$). Morever, the estimates inherite the robustness of the structure tensors (by averaging).

The one way wave equation can be solved by fast Fourier methods (FFT), and the computations needed for the tensor analysis are not significantly more expensive than those needed for the standard second order structure tensor. This is a consequence of the fact that the sizes of the tensors are only moderately increased. The separation of two ways in two variables requires the same amount of work as the eigenvalue decomposition needed for the standard structure tensor approach. Some more work is needed in the case of separating three intersecting waves (in three dimensions), but through a resultant method, it reduces to finding the roots of fourth degree polynomial in one variable (once coefficients are obtained through explicit expressions).

Once the local directions are estimated, a modified version of the one way way equation can be used to filter out the directions of interest. The idea is that if the oscillatory directions are known, then the way the corresponding waves propagate is also known (for short distances) . Hence, it is possible to account the displacement of the waves and compensate for this by moving the coordinate system in a similar manner. In this way, the waves with correct directions (i.e., with directions that agree with the obtained estimate) will remain stationary, while the waves with the wrong directions will propagate with time. A time averaging will thus cancel the undesired wave components.

Unfortunately, the deformation of the spatial coordinate system prevents the usage of ordinary FFT. However, this problem can be resolved by instead using algorithms for unequally spaced FFT [2, 5].

2. The one way wave equation. Let us consider the standard wave equation with constant velocity v_0,

$$u''_{tt} - v_0^2 \triangle u = 0. \tag{2.1}$$

Two initial conditions are needed to solve this equation. These are usually chosen by specifying function values at time zero, along with the first time derivative at time zero, i.e., $u(x,0) = f(x)$ and $u'_t(x,0) = g(x)$. First, let us consider the one-dimensional case $x \in \mathbb{R}$, and review how these initial conditions can be chosen such that the solution u consists of waves traveling in one direction only. Associated with these solutions is another (simpler) partial differential equation which has only one initial condition. This condition is of the type $u(x,0) = f(x)$. We will refer to this partial differential equation as the one-way wave equation. For the case of non-constant velocity, these partial different equation yield different solutions, but for the case of constant velocity the solutions coincide.

We use the following definition for the Fourier transform

$$\hat{f}(\xi) = \int f(x) \mathrm{e}^{-2\pi \mathrm{i} x \xi} \, dx,$$

and similarly for functions of several variables. Let us start by considering the one-dimensional version of (2.1),

$$u''_{tt} - v_0^2 u''_{xx} = 0. \tag{2.2}$$

By a Fourier transformation in the x-variable, we obtain

$$(\mathcal{F}_x u)''_{tt} + 4\pi^2 v_0^2 \mathcal{F}_x u = 0,$$

which have solutions of the form

$$(\mathcal{F}_x u)(\xi, t) = A^+(\xi)\mathrm{e}^{-2\pi \mathrm{i} v_0 \mathsf{sign}(\xi)|\xi|t} + A^-(\xi)\mathrm{e}^{2\pi \mathrm{i} v_0 \mathsf{sign}(\xi)|\xi|t} \tag{2.3}$$

$$= \widehat{A}^+(\xi)\mathrm{e}^{-2\pi \mathrm{i} v_0 \xi t} + \widehat{A}^-(\xi)\mathrm{e}^{2\pi \mathrm{i} v_0 \xi t}. \tag{2.4}$$

By an inverse Fourier transformation, we obtain (D'Lamberts principle)

$$u(x,t) = A^+(x,t) + A^-(x,t) = A^+(x - v_0 t) + A^-(x + v_0 t),$$

i.e., two waves traveling in the positive and negative x-directions, respectively. It is possible to eliminate one of these solutions by the choice of initial conditions. For instance, the problem

$$u''_{tt} - v_0^2 u''_{xx} = 0, \quad u(x,0) = f(x), \quad u'_t(x,0) = \mathcal{F}_x^{-1}(-2\pi \mathrm{i}\xi \widehat{f})(x),$$

will have the solution

$$u(x,t) = \mathcal{F}_x^{-1}(\mathcal{F}_x f \mathrm{e}^{-2\pi \mathrm{i} v_0 t \cdot})(x,t) = f(x - v_0 t).$$

In particular, for the case where

$$u_0(x) = \mathrm{e}^{2\pi \mathrm{i}\xi_0 x},$$

the solution is $u(x,t) = \mathrm{e}^{2\pi \mathrm{i}(\xi_0(x - v_0 t))}$. In other words, given an a pure oscillation with frequency ξ_0 as initial condition, the solution to the one-way wave equation yields a new pure oscillation with frequency $(\xi_0, \omega_0) = (\xi_0, -v_0\xi_0)$ in the extended domain (x,t).

A similar argument can be made in higher dimensions. Let us consider the q-dimensional case. Let $x = (x_1, \ldots, x_q)$. A Fourier transformation of (2.1) in the x-variables yields

$$(\mathcal{F}_x u)''_{tt} + 4\pi^2 \left(\sum_{l=1}^{q} \xi_l^2\right) v_0^2 (\mathcal{F}_x u) = 0.$$

There are several ways to choose the roots of $\sum_{l=1}^{q} \xi_l^2$. The pair of choices $\pm\mathsf{sign}(\xi_q)\sqrt{\sum_{l=1}^{q} \xi_l^2}$ gives solutions of the form

$$(\mathcal{F}_x u)(\xi) = \widehat{A}^+(\xi)\mathrm{e}^{-2\pi \mathrm{i} t\omega} + \widehat{A}^-(\xi)\mathrm{e}^{2\pi \mathrm{i} t\omega}, \quad \omega = \mathsf{sign}(\xi_q)\sqrt{\sum_{l=1}^{q} \xi_l^2},$$

which corresponds to waves traveling in the positive and negative x_q-direction, respectively. To see this, consider the choice of initial values

$$u(x,0) = f(x), \quad u'_t(x,0) = -2\pi \mathrm{i} \int \widehat{f}(\xi)\mathsf{sign}(\xi_q)\|\xi\|\mathrm{e}^{2\pi \mathrm{i}\langle x,\xi\rangle}\, d\xi.$$

As for the one-dimensional case, this choice forces $\widehat{A}^- = 0$, $\widehat{A}^+ = \widehat{f}$, and

$$\begin{aligned} u(x,t) &= \int_{\mathbb{R}} \int_{\mathbb{R}^{q-1}} \widehat{f}(\xi_1,\dots,\xi_{q-1},\xi_q) \mathrm{e}^{2\pi \mathrm{i}\left(\langle x,\xi\rangle - v_0 t \mathsf{sign}\xi_q \sqrt{\sum_{l=1}^q \xi_l^2}\right)} d\xi_1 \dots d\xi_{q-1} d\xi_q \\ &= \int_{\mathbb{R}^{q-1}} \mathrm{e}^{2\pi \mathrm{i} \sum_{l=1}^{q-1} x_l \xi_l} \left(\int_0^\infty \widehat{f}(\xi_1,\dots,\xi_{q-1},\xi_q) \mathrm{e}^{2\pi \mathrm{i}\left(x_q\xi_q - v_0 t \sqrt{\sum_{l=1}^q \xi_l^2}\right)} d\xi_q \right. \\ &\quad \left. + \int_{-\infty}^0 \widehat{f}(\xi_1,\dots,\xi_{q-1},\xi_q) \mathrm{e}^{2\pi \mathrm{i}\left(x_q\xi_q + v_0 t \sqrt{\sum_{l=1}^q \xi_l^2}\right)} d\xi_q \right) d\xi_1 \dots d\xi_{q-1}. \end{aligned}$$

A change of variable $\xi_q := -\xi_q$ in the second inner integral above combined with the fact that $\widehat{f}(\xi) = \overline{\widehat{f}(-\xi)}$ when u is real valued, yields

$$\begin{aligned} u(x,t) &= \int_{\mathbb{R}^{q-1}} \mathrm{e}^{2\pi \mathrm{i} \sum_{l=1}^{q-1} x_l \xi_l} \left(\int_0^\infty \widehat{f}(\xi_1,\dots,\xi_{q-1},\xi_q) \mathrm{e}^{2\pi \mathrm{i}\left(x_q\xi_q - v_0 t \sqrt{\sum_{l=1}^q \xi_l^2}\right)} d\xi_q \right. \\ &\quad \left. + \int_0^\infty \widehat{f}(\xi_1,\dots,\xi_{q-1},-\xi_q) \mathrm{e}^{2\pi \mathrm{i}\left(-x_q\xi_q + v_0 t \sqrt{\sum_{l=1}^q \xi_l^2}\right)} d\xi_q \right) d\xi_1 \dots d\xi_{q-1} \\ &= \int_0^\infty \int_{\mathbb{R}^{q-1}} \widehat{f}(\xi) \mathrm{e}^{2\pi \mathrm{i}\left(\langle x,\xi\rangle - v_0 t \sqrt{\sum_{l=1}^q \xi_l^2}\right)} d\xi_1 \dots d\xi_{q-1} d\xi_q \\ &\quad + \overline{\int_0^\infty \int_{\mathbb{R}^{q-1}} \widehat{f}(\xi) \mathrm{e}^{2\pi \mathrm{i}\left(\langle x,\xi\rangle - v_0 t \sqrt{\sum_{l=1}^q \xi_l^2}\right)} d\xi_1 \dots d\xi_{q-1} d\xi_q} \\ &= 2\mathsf{Re}\left(\int_0^\infty \int_{\mathbb{R}^{q-1}} \widehat{f}(\xi_1,\dots,\xi_{q-1},\xi_q) \mathrm{e}^{2\pi \mathrm{i}\left(\langle x,\xi\rangle - v_0 t \sqrt{\sum_{l=1}^q \xi_l^2}\right)} d\xi_1 \dots d\xi_{q-1} d\xi_q \right). \end{aligned}$$

We deduce that this corresponds to waves traveling in the positive x_q-direction by interpreting the above as a sum of plane waves with positive frequencies in the x_q-direction.

As for the scalar case, this solution takes the form of a oscillation with frequency Just as for the scalar case, this solution takes the form of a oscillation with frequency

$$(\xi_0, \omega_0) = \left(\xi_{0,1}, \dots, \xi_{0,q}, -v_0 \mathsf{sign}(\xi_{0,q}) \sqrt{\sum_{l=0}^q \xi_{0,l}^2} \right) \tag{2.5}$$

for $u_0(x,y) = \mathrm{e}^{2\pi \mathrm{i}(\langle \xi_0, \xi\rangle)}$. Hence, pure oscillations in the x domain transforms into pure oscillations in the extended domain (x,t). We introduce the one way wave operator $\mathcal{L} : C_0^\infty(\mathbb{R}^q) \mapsto C^\infty(\mathbb{R}^{q+1})$ through

$$u(x,t) = \mathcal{L} f(x,t) \tag{2.6}$$

$$= 2\mathsf{Re}\left(\int_0^\infty \int_{\mathbb{R}^{q-1}} \widehat{f}(\xi_1,\dots,\xi_{q-1},\xi_q) \mathrm{e}^{2\pi \mathrm{i}\left(\langle x,\xi\rangle - v_0 t \sqrt{\sum_{l=1}^q \xi_l^2}\right)} d\xi_1 \dots d\xi_{q-1} d\xi_q \right). \tag{2.7}$$

In Figure 1 we illustrate how the operator $\mathcal{L}$ acts on a simple function f consisting of two localized waves. As t evolves the localized waves move in different directions, and hence the point of intersection is moving. As the waves propagate, the phases at the intersections will change. We will make use of this fact in order to separate the waves.

3. Time extended structure tensors in two dimensionals. Definition 3.1. *Let f be a real-valued function of two variables, and let $u = \mathcal{L} f$. The structure tensor at scale $\alpha = (\alpha_1, \alpha_2, \alpha_3)$, $\alpha_j > 0$, $j = 1,2,3$, $T_\alpha(u) = T_\alpha(u)(x,y)$, is defined as*

$$T_\alpha(u)(x) = g_\alpha * (\nabla u)(\nabla u)^H(x) = \begin{pmatrix} g_\alpha * |u'_{x_1}|^2 & g_\alpha * u'_{x_1} \overline{u'_{x_2}} & g_\alpha * u'_{x_1} \overline{u'_t} \\ g_\alpha * u'_{x_2} \overline{u'_{x_1}} & g_\alpha * |u'_{x_2}|^2 & g_\alpha * u'_{x_2} \overline{u'_t} \\ g_\alpha * u'_t \overline{u'_{x_1}} & g_\alpha * u'_t \overline{u'_{x_2}} & g_\alpha * |u'_t|^2 \end{pmatrix} (x), \tag{3.1}$$

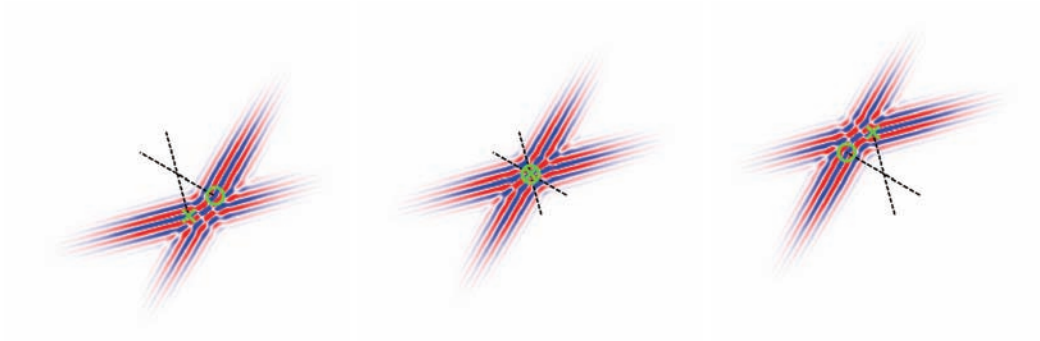

FIG. 1. *A simple example consisting of two localized waves with different orientations on which the one way operator $\mathcal{L}$ is applied. From left to right values of $\mathcal{L}f(x,t)$ is show for t negative, zero, and positive, respectively. Notice how the "intersection point" moves as t varies.*

where $*$ denotes convolution, $(\cdot)^H$ the conjugate (Hermitian) transpose, and where

$$g_\alpha = \frac{1}{\pi^{3/2}\alpha_1\alpha_2\alpha_3}\mathrm{e}^{-\frac{x_1^2}{\alpha_1^2}-\frac{x_2^2}{\alpha_2^2}-\frac{t^2}{\alpha_3^2}}.$$

LEMMA 3.2. *Let $f_j = c_j \mathsf{Re}\left(\mathrm{e}^{2\pi \mathrm{i}(x_1\xi_{j,1}+x_2\xi_{j,2})}\right)$, $\xi_{j,2} > 0$, $j = 1,2$. Let $f = f_1 + f_2$, and let $u = \mathcal{L}f$, $u_1 = \mathcal{L}f_1$, $u_2 = \mathcal{L}f_2$. Then*

$$\begin{aligned}\lim_{\|\alpha\|\to\infty} T_\alpha(u) &= \lim_{\|\alpha\|\to\infty} T_\alpha(u_1) + T_\alpha(u_2)\\ &= 4\pi^2\sum_{j=1}^{2}|c_j|^2\begin{pmatrix}\xi_{j,1}^2 & \xi_{j,1}\xi_{j,2} & \xi_{j,1}\sqrt{\xi_{j,1}^2+\xi_{j,2}^2}\\ \xi_{j,1}\xi_{j,2} & \xi_{j,2}^2 & \xi_{j,2}\sqrt{\xi_{j,1}^2+\xi_{j,2}^2}\\ \sqrt{\xi_{j,1}^2+\xi_{j,2}^2}\xi_{j,1} & \sqrt{\xi_{j,1}^2+\xi_{j,2}^2}\xi_{j,1} & \xi_{j,1}^2+\xi_{j,2}^2\end{pmatrix}\end{aligned}$$

Proof. The quadratic behavior of $T_\alpha(u)$ gives rise to elements of the form $g_\alpha * (|\xi_j|^2|u_j|^2)$ and cross terms $g_\alpha * (\xi_{1,1}\xi_{2,1}u_1\overline{u_2})$, respectively. For the first type, we have that

$$g_\alpha * (|\xi_{j,1}|^2|u_j|^2) = |c_j|^2|\xi_{j,1}|^2,$$

since $\|g_\alpha\|_1 = 1$. For the cross terms, it holds that

$$\begin{aligned}\xi_{1,1}\xi_{2,1}g_\alpha * (u_1\overline{u_2}) &= \xi_{1,1}\xi_{2,1}\mathrm{e}^{-\pi^2\left(\alpha_1^2(\xi_1-\xi_2)^2+\alpha_2^2(\eta_1-\eta_2)^2+\alpha_3^2\left(\sqrt{\xi_1^2+\eta_1^2}-\sqrt{\xi_2^2+\eta_2^2}\right)^2\right)}\\ &\to 0, \quad \|\alpha\|\to\infty.\end{aligned}$$

Hence, all of the cross terms will vanish as $\|\alpha\|\to\infty$. □

THEOREM 3.3. *Given the assumptions of Lemma 3.2, let $\lambda_k^\alpha(x)$, $e_k^\alpha(x)$, $k = 1,2,3$, $\lambda_1^\alpha \geq \lambda_2^\alpha \geq \lambda_3^\alpha$, be the eigenvalues and eigenvectors of $T_\alpha(u)$, respectively, at each point x. Moreover, let*

$$W^\alpha = \begin{pmatrix} e_{1,3}^\alpha e_{2,3}^\alpha & (e_{2,3}^\alpha)^2 - v_0^2(e_{3,3}^\alpha)^2 \\ -(e_{1,3}^\alpha)^2 + v_0^2(e_{3,3}^\alpha)^2 & -e_{1,3}^\alpha e_{2,3}^\alpha \end{pmatrix},$$

and let ξ_j^α, $j = 1,2$, be eigenvectors of W^α. Then

$$\lim_{\alpha\to 0}\lambda_3^\alpha = 0,$$

and

$$\lim_{\alpha\to 0} \xi_j^\alpha = \xi_{I(j)}, \quad j = 1, 2,$$

where I is a permutation operator.

Proof. Introduce $W = \lim_{\|\alpha\|\to\infty} W^\alpha$ and let $e_3 = \lim_{\|\alpha\|\to\infty} e_3^\alpha$. It follows from Lemma 3.2 that $\lim_{\alpha\to\infty} T_\alpha(u)$ is a rank 2 tensor, proving the first claim of the theorem. Moreover, as $\lim_{\alpha\to\infty} T_\alpha(u) = \lim_{\alpha\to\infty} T_\alpha(u_1) + \lim_{\alpha\to\infty} T_\alpha(u_2)$ it follows that e_3 is orthogonal to ∇u_j, $j = 1, 2$, i.e.,

$$\xi_{j,1} e_{1,1} + \xi_{j,2} e_{2,1} - v_0 \sqrt{\xi_{j,1}^2 + \xi_{j,2}^2}\, e_{3,3} = 0, \quad j = 1, 2.$$

By rearranging terms and squaring, the equation

$$\begin{pmatrix} \xi_{j,1} & \xi_{j,2} \end{pmatrix} \begin{pmatrix} e_{1,3}^2 - v_0^2 e_{3,3}^2 & e_{1,3} e_{2,3} \\ e_{1,3} e_{2,3} & e_{2,3}^2 - v_0^2 e_{3,3}^2 \end{pmatrix} \begin{pmatrix} \xi_{j,1} \\ \xi_{j,2} \end{pmatrix} = 0, \quad j = 1, 2,$$

is obtained. The solutions to this quadratic equation are given by the eigenvectors of W, since if ξ_j is an eigenvector to W with eigenvalue μ_j, then

$$\begin{aligned} &\xi_j^{\mathbb{T}} \begin{pmatrix} e_{1,3} e_{2,3} & e_{2,3}^2 - v_0^2 e_{3,3}^2 \\ -e_{1,3}^2 + v_0^2 e_{3,3}^2 & -e_{1,3} e_{2,3} \end{pmatrix} \xi_j \\ &= \begin{pmatrix} \xi_{j,2} & -\xi_{j,1} \end{pmatrix} \begin{pmatrix} e_{1,3}^2 - v_0^2 e_{3,3}^2 & e_{1,3} e_{2,3} \\ e_{1,3} e_{2,3} & e_{2,3}^2 - v_0^2 e_{3,3}^2 \end{pmatrix} \begin{pmatrix} \xi_{j,1} \\ \xi_{j,2} \end{pmatrix} \\ &= \begin{pmatrix} \xi_{j,2} & -\xi_{j,1} \end{pmatrix} \mu_j \begin{pmatrix} \xi_{j,1} \\ \xi_{j,2} \end{pmatrix} = 0. \end{aligned}$$

□

We end this section by an example illustrating the directionality estimation. As f we have used a part of a synthetic seismic data set. The data set has been extented by the one-way wave equation, and the structure tensor (3.1) is computed from the extention. Using Theorem 3.3 directions fields $\xi_1(x)$ and $\xi_2(x)$ are computed and used as local frequency estimations. In two dimensions, the fields $\xi_1(x)$ and $\xi_2(x)$ can be illustrated by means of angles, and these are depicted in the top panels of Figure 2. Recall that the fields can only be recovered up to some permutation. One choice of ordering for illustration purposes would be by the "amplitude" of which the two components contribute to the rank two tensor (3.1). However, this can easily cause discontinuities at points where the strength of the events switches from one to the other. Hence, this choice of ordering can be difficult to interpret when depicted as images. Therefore, an ordering in angle is instead used in the examples that follow. In the lower panel of Figure 2, the data set f is shown with an overlayed quiver plot. The quiver plots show the estimated directions $\xi_1(x)$ and $\xi_2(x)$ in blue and red, respectively. Notice, for instance, the parts in the middle where two waves with different directions overlap, and how they are distinguished.

4. Recovering wave components. Once directions ξ_j, $j = 1, \ldots, q$ are estimated, we turn focus to constructing a method for separating the different components. One approach to do this could be by computing derivatives and making local changes of coordinates to try to separate the components. This is a fast and simple approach, but it may be undesirable due to the sensitivity to noise inherited by numerical differentiation. We propose a different approach, where again the one way wave equation is used, this time to filter out the directionality components.

Given a directionality function $\theta(x)$ (for instance of of the estimations ξ_j), let

$$\mathcal{G}_\theta f(x) = \frac{2\sqrt{\beta}}{\sqrt{\pi}} \int_{-\infty}^{\infty} \mathsf{Re} \left(\int_0^\infty \int_{\mathbb{R}^{q-1}} \widehat{f}(\xi) \mathrm{e}^{2\pi \mathrm{i} \left(\left\langle x + t v_0 \frac{\theta(x)}{\|\theta(x)\|}, \xi \right\rangle - t v_0 \|\xi\| \right)} d\xi_1 \ldots d\xi_q \right) \mathrm{e}^{-\beta t^2} dt, \tag{4.1}$$

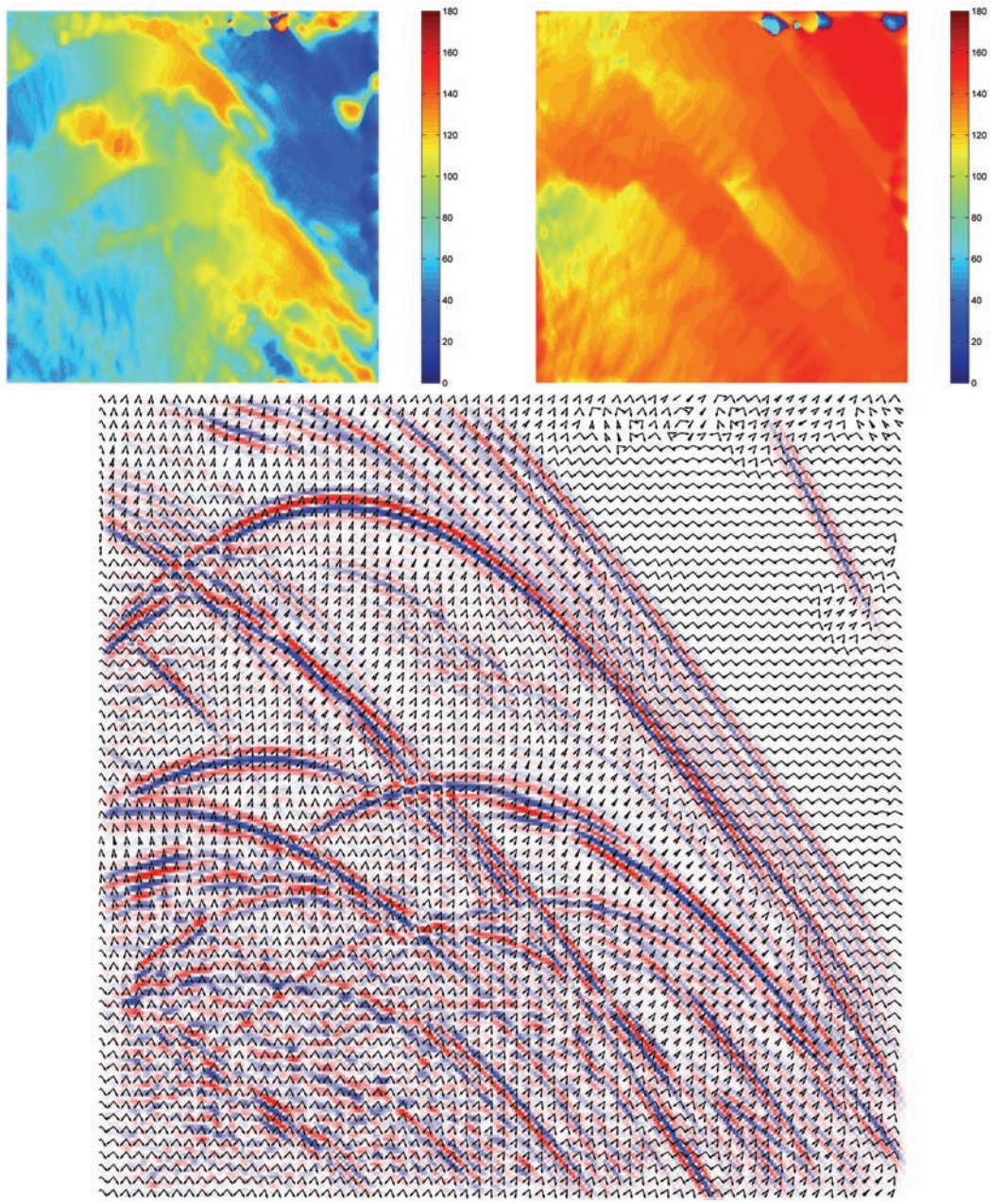

FIG. 2. *The two top panels show estimated angles of direction, and the lower panel show the data f with a quiver plots of the directionality overlayed*

where $\beta > 0$. This operator have the following interpretation: waves are propagated forward by the phase term $-tv_0\|\xi\|$, but at the same time they are propagated backwards in the direction specified by $\theta(x)$ due to the factor $tv_0\theta(x)$ in $\langle x+tv_0\theta(x), \xi\rangle$. The total effect is thus that waves with direction that coincides with θ will not propagate with time, while other waves will. Due to the averaging time integral, waves with the wrong direction will tend to cancel out, and only the parts with the desired directionality will remain. This interpretation is illustrated in Figure 3. We can see how parts of the waves remain at the same location, while other parts move. For regions where there are two (distinct) directions, the parts that move and the parts that remain at the same location

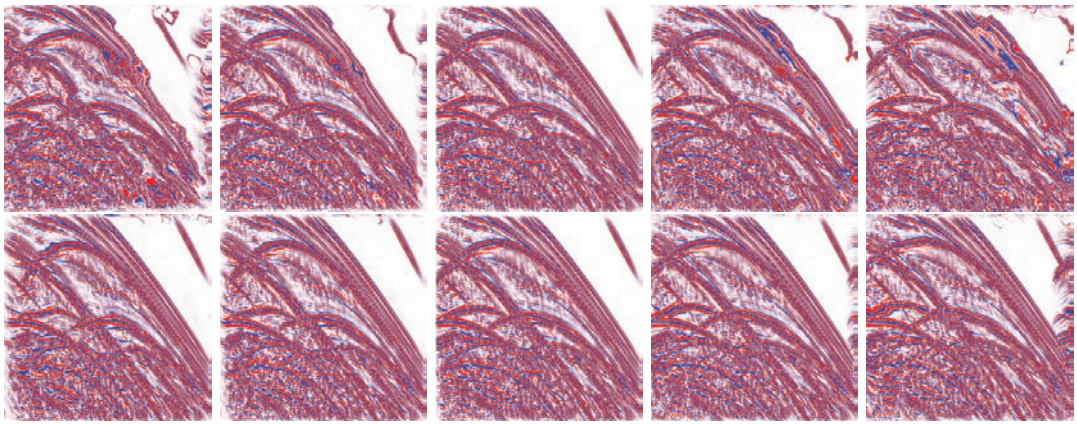

FIG. 3. *Illustration of how the operator (4.1) works. The effect of applying the inner integrals for different values of time (from left to right) for $\theta(x) = \xi_1(x)$ and $\theta(x) = \xi_2(x)$ in the upper and lower panels, respectively. Here, the estimated values of $\xi_j(x)$, $j = 1, 2$ were used. When averaging in time, the undesired waves will be filter out.*

interchange places between the upper and the lower panels.

In Figure 4 the total result of (4.1) (that is the effect after a weighted averaging of the panels in Figure 3 from left to right) First, estimations of $\xi_1(x)$ and $\xi_2(x)$ are obtained through the procedure described in section 3. The original data f is depicted in the top left panel of Figure 4. The estimates of $\xi_1(x)$ and $\xi_2(x)$ are then used to compute $\mathcal{G}_{\xi_1} f$ and $\mathcal{G}_{\xi_2} f$. The results are show in the two lower panel of Figure 4. One can clearly see how the contributions from waves with different directions tend to separate between $\mathcal{G}_{\xi_1} f$ and $\mathcal{G}_{\xi_2} f$, as desired. At places x where there is only one distinct direction, $\xi_1(x)$ and $\xi_2(x)$ become close to parallel, and the reconstructions coincide. This situation can cause problems with degenerate solutions of (3.1). However, such cases can be recognized by inspection of the singular values of $T_\alpha(u)(x)$, for instance by using some threshold level to determine whether there are one or two directions that contribute at a certain point x.

Let us consider a schematic implementation based on fast Fourier transforms in two dimensions. To simplify the presentation we will ignore the well known effects of boundary conditions as well as problems related to sampling density. Assume that f have essential (numerical) support on $[-1/2, 1/2] \times [-1/2, 1/2]$, and that it is sampled (sufficiently dense) on an equally spaced grid

$$X = \left\{ \frac{j}{N} : j \in \mathbb{Z}^2, -\frac{N}{2} \le j_1 < \frac{N}{2}, \quad -\frac{N}{2} \le j_2 < \frac{N}{2} \right\}.$$

Let

$$F(k) = \frac{1}{N^2} \sum_{j \in X} f(j) \mathrm{e}^{-2\pi \mathrm{i} \langle j, k \rangle}, \quad k \in \Xi,$$

where

$$\Xi = \left\{ k : k \in \mathbb{Z}^2, -\frac{N}{2} \le k_1 < \frac{N}{2}, \quad -\frac{N}{2} \le k_2 < \frac{N}{2} \right\}.$$

The assumptions above are to ensure that F is a good approximation of $\widehat{f}$ on Ξ.

The action of the operator $\mathcal{L}$ in (2.6) for a fixed time t can then be implemented by means of the multiplication of a phase factor

$$H(k, t) = F(k) \mathrm{e}^{-2\pi \mathrm{i} v_0 t \sqrt{k_1^2 + k_2^2}} \tag{4.2}$$

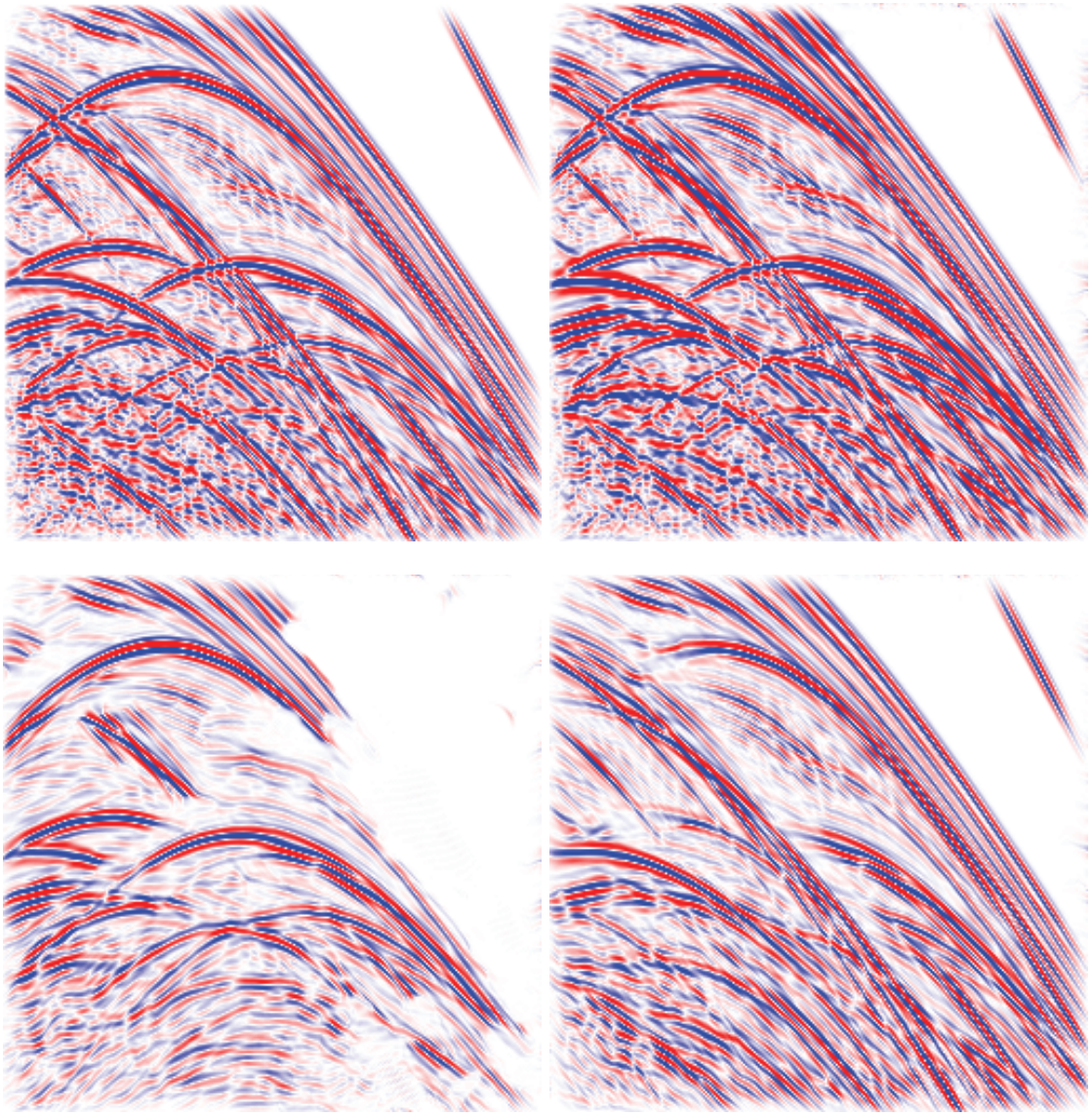

FIG. 4. *Illustration of the total effect of the operator (4.1) in two dimensions. The upper left panel show the original f, and the two lower panel show $\mathcal{G}_{\xi_1} f$ and $\mathcal{G}_{\xi_2} f$. The upper right panel shows $\mathcal{G}_{\xi_1} f + \mathcal{G}_{\xi_2} f$. The same thresholded gray scale is used for all four images.*

followed by an inverse discrete Fourier transform

$$u(j,t) = 2\mathsf{Re}\left(\sum_{k\in\Xi} H(k,t)\mathrm{e}^{2\pi\mathrm{i}\langle j,k\rangle}\right), \quad j \in X.$$

The implementation of $\mathcal{G}_\theta$ is a bit more delicate than a first glance may indicate. Whereas the operator $\mathcal{L}$ can be implemented in a fast manner by using multiplication in the frequency domain through standard FFT, the fact that we need to correct for the spatial displacement in x (i.e. replace x by $x + v_0 t \frac{\theta(x)}{\|\theta(x)\|}$) prevents the usage of standard FFT for the inverse transform step. To see this,

let H be as in (4.2) and apply the (approximate) inverse Fourier transform

$$\sum_{k\in\Xi}\tilde{H}(k,t)\mathrm{e}^{2\pi\mathrm{i}\left(\left(j_1+\left(tv_0\frac{\theta(x)}{\|\theta(x)\|}\right)_1\right)k_1+\left(j_2+\left(tv_0\frac{\theta(x)}{\|\theta(x)\|}\right)_2\right)k_2\right)}.$$

The sum above is no longer of the form of a discrete Fourier transform, and hence the FFT can not be used to compute the sum fast. However, sums of this type can be rapidly computed by means of unequally spaced fast Fourier transforms (USFFT) [2, 5].

The operator $\mathcal{G}_\theta$ of (4.1) can alternatively be interpreted in terms of pseudo-differential operators. To see this, note that

$$\begin{aligned}\mathcal{G}_\theta f(x) &= \frac{2\sqrt{\beta}}{\sqrt{\pi}}\mathsf{Re}\left(\int_0^\infty\int_{\mathbb{R}^{q-1}}\widehat{f}(\xi)\mathrm{e}^{2\pi\mathrm{i}\langle x,\xi\rangle}\int_{-\infty}^{\infty}\mathrm{e}^{-\beta t^2+2\pi\mathrm{i}tv_0\left(\left\langle\frac{\theta(x)}{\|\theta(x)\|},\xi\right\rangle-\|\xi\|\right)}dt\ d\xi_1\dots d\xi_q\right)\\ &= 2\mathsf{Re}\left(\int_0^\infty\int_{\mathbb{R}^{q-1}}\widehat{f}(\xi)\mathrm{e}^{2\pi\mathrm{i}\langle x,\xi\rangle}\mathrm{e}^{-\frac{\pi^2}{\beta}v_0^2\left(\left\langle\theta(x),\xi\right\rangle-\|\xi\|\right)^2}\ d\xi_1\dots d\xi_q\right)\\ &= 2\mathsf{Re}\left(\int_0^\infty\int_{\mathbb{R}^{q-1}}\widehat{f}(\xi)\mathrm{e}^{2\pi\mathrm{i}\langle x,\xi\rangle}\mathrm{e}^{-\frac{\pi^2}{\beta}v_0^2\|\xi\|^2\left(1-\frac{\langle\theta(x),\xi\rangle}{\|\xi\|\|\theta x\|}\right)^2}\ d\xi_1\dots d\xi_q\right).\end{aligned}$$

This operator is thus closely related to the pseudo differential operator P_θ with symbol

$$p(x,\xi)=\mathrm{e}^{-\frac{\pi^2}{\beta}v_0^2\|\xi\|^2\left(1-\frac{\langle\theta(x),\xi\rangle}{\|\xi\|\|\theta x\|}\right)^2},$$

which suppresses high frequency information with Gaussian factors where the width of the Gaussian is determined by the angle between ξ and θ_x. A potential alternative to implementing $\mathcal{G}_\theta$ by means of the one way wave equation (using USFFT), could be to construct a fast method of computing pseudo differential operators of the type above[1].

5. Time extended structure tensors in three dimensions. For the three dimensional problem, it is natural to consider functions (locally) of the form

$$f(x)=\sum_{j=1}^{3}c_j\mathrm{e}^{2\pi\mathrm{i}\langle x,\xi\rangle},$$

and the separation problem of recovering the directions (frequencies) ξ_j. In contrast to the two-dimensional case, it turns out that extending f into a function of space and time ($u(x,t)=\mathcal{L}f(x,t)$) does not provide sufficient information to recover ξ_j from the structure tensor. However, by extending the data using two "time" variables, it turns out that enough information is available. There are several ways to do this generalization. One choice is

$$\mathcal{L}f(x,t)=2\mathsf{Re}\left(\int_0^\infty\int_{\mathbb{R}^2}\int_{\mathbb{R}^3}f(y)\mathrm{e}^{2\pi\mathrm{i}\left(\langle x-y,\xi\rangle-t_1v_1\sqrt{\xi_1^2+\xi_2^2+\xi_3^2}-t_2v_2\sqrt{\xi_1^2+\xi_3^2}\right)}\,dy\,d\xi_1d\xi_2d\xi_3\right),$$

where v_1 and v_2 are constants. For t_2 fixed, $\mathcal{L}u(x,t)$ corresponds to the one way wave equation (moving in the positive x_3 direction) in three dimensions, while for t_1 fixed $\mathcal{L}u(x,t)$ corresponds to solutions to the one way wave equation (moving in the positive x_3 direction) in two dimensional slices (x_1,x_3).

In a similar spirit as for the two-dimensional case, we introduce structure tensors

$$\begin{aligned}T_\alpha(u)(x) &= g_\alpha*(\nabla u)(\nabla u)^H(x)\\ &= g_\alpha*\begin{pmatrix}|u'_{x_1}|^2 & u'_{x_1}\overline{u'_{x_2}} & u'_{x_1}\overline{u'_{x_3}} & u'_{x_1}\overline{u'_{t_1}} & u'_{x_1}\overline{u'_{t_2}}\\ u'_{x_2}\overline{u'_{x_1}} & |u'_{x_2}|^2 & u'_{x_2}\overline{u'_{x_3}} & u'_{x_2}\overline{u'_{t_1}} & u'_{x_2}\overline{u'_{t_2}}\\ u'_{x_3}\overline{u'_{x_1}} & u'_{x_3}\overline{u'_{x_2}} & |u'_{x_3}|^2 & u'_{x_3}\overline{u'_{t_1}} & u'_{x_3}\overline{u'_{t_2}}\\ u'_{t_1}\overline{u'_{x_1}} & u'_{t_1}\overline{u'_{x_2}} & u'_{t_1}\overline{u'_{x_3}} & |u'_{t_1}|^2 & u'_{t_1}\overline{u'_{t_2}}\\ u'_{t_2}\overline{u'_{x_1}} & u'_{t_2}\overline{u'_{x_2}} & u'_{t_2}\overline{u'_{x_3}} & u'_{t_2}\overline{u'_{t_1}} & |u'_{t_2}|^2\end{pmatrix}(x).\end{aligned}$$

[1] I am, however, not aware of any existing method to do this.

Lemma 3.2 is directly generalized to the three dimensional setting.

The results for the two-dimensional case can now be generalized to the three dimensional case.

THEOREM 5.1. *Let* $f_j = c_j \mathsf{Re}\left(\mathrm{e}^{2\pi \mathrm{i}\langle x,\xi_j\rangle}\right)$, $\xi_{j,3} > 0$, $u_j = \mathcal{L}f_j$, $j = 1,2,3$. *Form* $f = \sum_{j=1}^{3} f_j$, *and let* $u = \mathcal{L}f$. *Then*

$$
\begin{aligned}
T(u) := \lim_{\|\alpha\|\to\infty} T_\alpha(u) &= \sum_{j=1}^{3} \lim_{\|\alpha\|\to\infty} T_\alpha(u_j) \\
&= 4\pi^2 \sum_{j=1}^{3} |c_j|^2 \begin{pmatrix} \xi_{j,1}^2 & \xi_{j,1}\xi_{j,2} & \xi_{j,1}\xi_{j,3} & \xi_{j,1}\omega_{j,1} & \xi_{j,1}\omega_{j,2} \\ \xi_{j,2}\xi_{j,1} & \xi_{j,2}^2 & \xi_{j,2}\xi_{j,3} & \xi_{j,2}\omega_{j,1} & \xi_{j,2}\omega_{j,2} \\ \xi_{j,3}\xi_{j,1} & \xi_{j,3}\xi_{j,2} & \xi_{j,3}^2 & \xi_{j,3}\omega_{j,1} & \xi_{j,3}\omega_{j,2} \\ \omega_{j,1}\xi_{j,1} & \omega_{j,1}\xi_{j,2} & \omega_{j,1}\xi_{j,3} & \omega_{j,1}^2 & \omega_{j,1}\omega_{j,2} \\ \omega_{j,2}\xi_{j,1} & \omega_{j,2}\xi_{j,2} & \omega_{j,2}\xi_{j,3} & \omega_{j,2}\omega_{j,1} & \omega_{j,2}^2 \end{pmatrix},
\end{aligned} \tag{5.1}
$$

where

$$
\omega_1 = -v_1\sqrt{\xi_{j,1}^2 + \xi_{j,2}^2 + \xi_{j,3}^2}, \quad \omega_2 = -v_2\sqrt{\xi_{j,1}^2 + \xi_{j,3}^2}. \tag{5.2}
$$

Let $\lambda_k^\alpha(x)$, $e_k^\alpha(x)$, $k = 1,\ldots,5$, $\lambda_1^\alpha \geq \lambda_2^\alpha \geq \lambda_3^\alpha$, *be the eigenvalues and eigenvectors of* $T_\alpha(u)$, *respectively, at each point* x. *Moreover, let*

$$
\begin{aligned}
w_1^\alpha &= e_4^\alpha - e_5^\alpha \frac{e_{5,4}}{e_{5,5}}, \quad w_1 = \lim_{\|\alpha\|\to\infty} w_1^\alpha, \\
w_2^\alpha &= e_4^\alpha - e_5^\alpha \frac{e_{4,4}}{e_{4,5}}, \quad w_2 = \lim_{\|\alpha\|\to\infty} w_2^\alpha.
\end{aligned}
$$

Then

$$
\lim_{\alpha\to 0} \lambda_4^\alpha = \lim_{\alpha\to 0} \lambda_5^\alpha = 0, \tag{5.3}
$$

and ξ_j *are solutions to homogeneous quadratic system*

$$
\begin{aligned}
&\begin{pmatrix} \xi_{j,1} & \xi_{j,2} & \xi_{j,3} \end{pmatrix} \begin{pmatrix} w_{1,1}^2 - v_1^2 w_{4,1}^2 & w_{1,1}w_{2,1} & w_{1,1}w_{3,1} \\ w_{2,1}w_{1,1} & w_{2,1}^2 - v_1^2 w_{4,1}^2 & w_{2,1}w_{3,1} \\ w_{3,1}w_{1,1} & w_{3,1}w_{2,1} & w_{3,1}^2 - v_1^2 w_{4,1}^2 \end{pmatrix} \begin{pmatrix} \xi_{j,1} \\ \xi_{j,2} \\ \xi_{j,3} \end{pmatrix} = 0, \\
&\begin{pmatrix} \xi_{j,1} & \xi_{j,2} & \xi_{j,3} \end{pmatrix} \begin{pmatrix} w_{1,2}^2 - v_2^2 w_{5,2}^2 & w_{1,2}w_{2,2} & w_{1,2}w_{3,2} \\ w_{2,2}w_{1,2} & w_{2,2}^2 & w_{2,2}w_{3,2} \\ w_{3,2}w_{1,2} & w_{3,2}w_{2,2} & w_{3,2}^2 - v_2^2 w_{5,2}^2 \end{pmatrix} \begin{pmatrix} \xi_{j,1} \\ \xi_{j,2} \\ \xi_{j,3} \end{pmatrix} = 0.
\end{aligned} \tag{5.4}
$$

Proof. The proof of (5.1) is similar as the proof of Lemma 3.2. The result (5.3) thus follows as (5.1) is clearly a rank three tensor. Using (5.1) with (5.2) in combination that $w_{5,1} = w_{4,2} = 0$ by construction, gives

$$
\begin{aligned}
(\xi_{j,1}w_{1,1} + \xi_{j,2}w_{1,1} + \xi_{j,3}w_{1,1})^2 &= v_1 w_{4,1}\sqrt{\xi_{j,1}^2 + \xi_{j,2}^2 + \xi_{j,3}^2} \\
(\xi_{j,1}w_{1,2} + \xi_{j,2}w_{1,2} + \xi_{j,3}w_{1,2})^2 &= v_2 w_{5,1}\sqrt{\xi_{j,1}^2 + \xi_{j,3}^2},
\end{aligned}
$$

which after squaring and rearrangement of terms yields (5.4). ∎ For the sake of completeness, we provide an explicit way to solve (5.4). Since it is a homogeneous system, $\lambda\xi_j$ will solve (5.4) whenever ξ_j does so. From (5.1) this corresponds to the fact that it is not possible to distinguish the contribution from $\|\xi_j\|$ from the contribution of the amplitude $|c_j|$. Because of this fact, we may set $\xi_{j,3} = 1$, and obtain a system of two polynomial of degree two in two variables,

$$
\begin{aligned}
p_1(\xi_1,\xi_2) &= a_{1,1}\xi_1^2 + a_{1,2}\xi_1\xi_2 + a_{2,2}\xi_2^2 + a_{1,0}\xi_1 + a_{2,0}\xi_2 + a_{0,0} = 0 \\
p_1(\xi_1,\xi_2) &= b_{1,1}\xi_1^2 + b_{1,2}\xi_1\xi_2 + b_{2,2}\xi_2^2 + b_{1,0}\xi_1 + b_{2,0}\xi_2 + b_{0,0} = 0,
\end{aligned} \tag{5.5}
$$

where

$$\begin{aligned}
&a_{1,1} = w_{1,1}^2 - v_1^2 w_{4,1}^2, && a_{1,2} = 2w_{1,1}w_{2,1}, && a_{2,2} = w_{2,1}^2 - v_1^2 w_{4,1}^2,\\
&a_{1,0} = 2w_{1,1}w_{3,1}, && a_{2,0} = 2w_{2,1}w_{3,1}, && a_{0,0} = w_{3,1}^2 - v_1^2 w_{4,1}^2,\\
&b_{1,1} = w_{1,2}^2 - v_2^2 w_{5,2}^2, && b_{1,2} = 2w_{1,2}w_{2,2}, && b_{2,2} = w_{2,2}w_{1,2},\\
&b_{1,0} = 2w_{1,2}w_{3,2}, && b_{2,0} = 2w_{2,2}w_{3,2}, && b_{0,0} = w_{3,2}^2 - v_2^2 w_{5,2}^2.
\end{aligned}$$

This system have four roots by Bezouts theorem [4]. It can for instance be solved by using resultants, [4]. An alternative could be to used u-resultants, for which well conditioned methods are developed in [11]. For fixed ξ_1, a necessary condition for $p_1(\xi_1,\xi_2) = p_{2,1}\xi_2^2 + p_{1,1}\xi_2 + p_{0,1} = 0$ and $p_2(\xi_1,\xi_2) = p_{2,2}\xi_2^2 + p_{1,2}\xi_2 + p_{0,2} = 0$ to have a common root (in ξ_2) is that

$$\begin{vmatrix} p_{2,1} & p_{1,1} & p_{0,1} & 0 \\ 0 & p_{2,1} & p_{1,1} & p_{0,1} \\ p_{2,2} & p_{1,2} & p_{0,2} & 0 \\ 0 & p_{2,2} & p_{1,2} & p_{0,2} \end{vmatrix} = 0.$$

From this constraint we obtain equations for eligable values of ξ_1, i.e.,

$$\begin{aligned}
&\begin{vmatrix} a_{2,2} & a_{1,2}\xi_1 + a_{2,0} & a_{1,1}\xi_1^2 + a_{1,0}\xi_1 + a_{0,0} & 0 \\ 0 & a_{2,2} & a_{1,2}\xi_1 + a_{2,0} & a_{1,1}\xi_1^2 + a_{1,0}\xi_1 + a_{0,0} \\ b_{2,2} & b_{1,2}\xi_1 + b_{2,0} & b_{1,1}\xi_1^2 + b_{1,0}\xi_1 + b_{0,0} & 0 \\ 0 & b_{2,2} & b_{1,2}\xi_1 + b_{2,0} & b_{1,1}\xi_1^2 + b_{1,0}\xi_1 + b_{0,0} \end{vmatrix}\\
&\qquad = d_4\xi_1^4 + d_3\xi_1^3 + d_2\xi_1^2 + d_1\xi_1 + d_0 = 0.
\end{aligned}$$

where

$$\begin{aligned}
d_4 =& a_{2,2}b_{1,2}^2a_{1,1} + b_{2,2}a_{1,2}^2b_{1,1} - a_{2,2}b_{1,2}a_{1,2}b_{1,1} - 2a_{2,2}b_{2,2}b_{1,1}a_{1,1}\\
&- b_{2,2}a_{1,2}b_{1,2}a_{1,1} + a_{2,2}^2b_{1,1}^2 + b_{2,2}^2a_{1,1}^2,\\
d_3 =& 2a_{2,2}^2b_{1,1}b_{1,0} + a_{2,2}b_{1,2}^2a_{1,0} + 2b_{2,2}^2a_{1,1}a_{1,0} + b_{2,2}a_{1,2}^2b_{1,0} + 2a_{2,2}b_{1,2}b_{2,0}a_{1,1}\\
&- a_{2,2}b_{1,2}a_{1,2}b_{1,0} - a_{2,2}b_{1,2}a_{2,0}b_{1,1} - a_{2,2}b_{2,0}a_{1,2}b_{1,1} - 2a_{2,2}b_{2,2}b_{1,1}a_{1,0}\\
&- 2a_{2,2}b_{2,2}b_{1,0}a_{1,1} + 2b_{2,2}a_{1,2}a_{2,0}b_{1,1} - b_{2,2}a_{1,2}b_{1,2}a_{1,0} - b_{2,2}a_{1,2}b_{2,0}a_{1,1}\\
&- b_{2,2}a_{2,0}b_{1,2}a_{1,1},\\
d_2 =& 2a_{2,2}^2b_{1,1}b_{0,0} + a_{2,2}b_{1,2}^2a_{0,0} + a_{2,2}b_{2,0}^2a_{1,1} + 2b_{2,2}^2a_{1,1}a_{0,0} + b_{2,2}a_{1,2}^2b_{0,0}\\
&+ b_{2,2}a_{2,0}^2b_{1,1} + 2a_{2,2}b_{1,2}b_{2,0}a_{1,0} - a_{2,2}b_{1,2}a_{1,2}b_{0,0} - a_{2,2}b_{1,2}a_{2,0}b_{1,0}\\
&- a_{2,2}b_{2,0}a_{1,2}b_{1,0} - a_{2,2}b_{2,0}a_{2,0}b_{1,1} - 2a_{2,2}b_{2,2}b_{1,1}a_{0,0} - 2a_{2,2}b_{2,2}b_{1,0}a_{1,0}\\
&- 2a_{2,2}b_{2,2}b_{0,0}a_{1,1} + 2b_{2,2}a_{1,2}a_{2,0}b_{1,0} - b_{2,2}a_{1,2}b_{1,2}a_{0,0} - b_{2,2}a_{1,2}b_{2,0}a_{1,0}\\
&- b_{2,2}a_{2,0}b_{1,2}a_{1,0} - b_{2,2}a_{2,0}b_{2,0}a_{1,1} + a_{2,2}^2b_{1,0}^2 + b_{2,2}^2a_{1,0}^2,\\
d_1 =& 2a_{2,2}^2b_{1,0}b_{0,0} + a_{2,2}b_{2,0}^2a_{1,0} + 2b_{2,2}^2a_{1,0}a_{0,0} + b_{2,2}a_{2,0}^2b_{1,0} + 2a_{2,2}b_{1,2}b_{2,0}a_{0,0}\\
&- a_{2,2}b_{1,2}a_{2,0}b_{0,0} - a_{2,2}b_{2,0}a_{1,2}b_{0,0} - a_{2,2}b_{2,0}a_{2,0}b_{1,0} - 2a_{2,2}b_{2,2}b_{1,0}a_{0,0}\\
&- 2a_{2,2}b_{2,2}b_{0,0}a_{1,0} + 2b_{2,2}a_{1,2}a_{2,0}b_{0,0} - b_{2,2}a_{1,2}b_{2,0}a_{0,0} - b_{2,2}a_{2,0}b_{1,2}a_{0,0}\\
&- b_{2,2}a_{2,0}b_{2,0}a_{1,0},\\
d_0 =& - a_{2,2}b_{2,0}a_{2,0}b_{0,0} - 2a_{2,2}b_{2,2}b_{0,0}a_{0,0} - b_{2,2}a_{2,0}b_{2,0}a_{0,0} + a_{2,2}b_{2,0}^2a_{0,0}\\
&+ b_{2,2}a_{2,0}^2b_{0,0} + a_{2,2}^2b_{0,0}^2 + b_{2,2}^2a_{0,0}^2.
\end{aligned}$$

The ξ_1-component of the four roots can be obtained by solving this (one variable) polynomial of degree four. Once the ξ_1 components are know, the ξ_2 components can easily be recovered from (5.5).

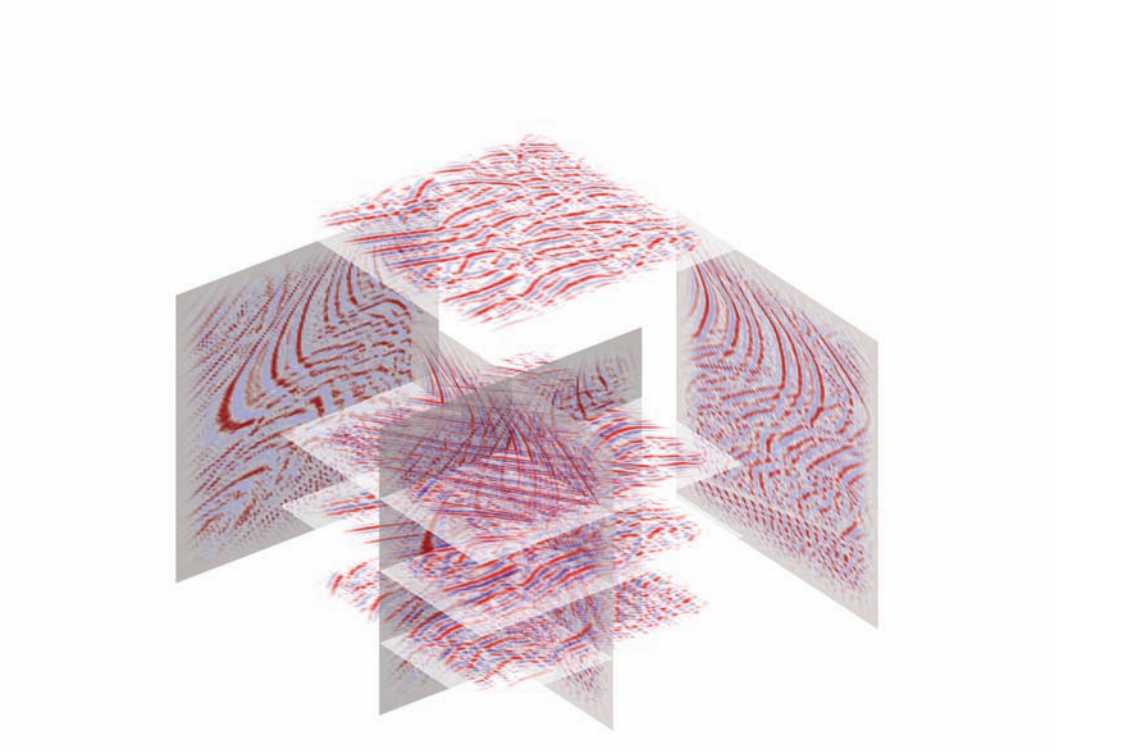

FIG. 5. *A three dimensional volume of synthetic seismic data shown with volume slices*

6. Three dimensional processing. Figure 5 shows a three dimensional volume of synthetic seismic data. This data set is fairly complicated, despite the fact that it is syntetic data set, i.e., obtained as a numerical solution to a partial differential equation instead of originating from real measurements. When visualized in two dimensions it can be hard to see the local wave structure. A visual analysis of data sets like this requires more user interaction than in the two dimensional case. An automated method for separating wave could therefore be useful. We will not try to construct such a method in this work, but note that the suggested procedure of directionality estimation could serve as a useful tool for constructing such automated methods.

The three mid slices $x_1 = 0$, $x_2 = 0$ and $x_3 = 0$ are shown in shifted locations in Figure 5. For illustration purposes, we will concentrate on results from one of the slices, the $x_3 = 0$ slice. Figure 6 shows the processing result for this slice. The original data slice is shown as an image in the top left panel. The right top panel shows the sum of the three components $\mathcal{G}_{\xi_1} f$, $\mathcal{G}_{\xi_2} f$ and $\mathcal{G}_{\xi_3} f$, where the color scale have been normalized to that of the original slice. Not all regions of the data have three distinguishable components. At these places, the estimated directions may be rather similar. Such regions could for instance be identified from some rule that depends on the eigenvalues of $T_\alpha(u)$ in (5.1), for instance thresholding. For such (degenerated) cases, it would be possible to use the equations for the two dimensional case to determine two (local) directions, and even simpler for the rank one case. The problem with this approach is to determine a good rule (threshold level) for determining when one of the eigenvalues of $T_\alpha(u)$ are to be considered to be discardable. Instead, we have chosen to detect three directions at each point, and to reduce them to two directions at points where two of them become sufficiently close to being parallel. For this simulation we have reduced the number of directions if cosine of the angle between two them are above 0.8.

The middle panels of Figure 6 shows $\mathcal{G}_{\xi_1} f$, $\mathcal{G}_{\xi_2} f$ and $\mathcal{G}_{\xi_3} f$, respectively. The white areas of the middle right panels are regions where two of the estimated directions had an angle between them with a cosine value larger than 0.8. The lower panels of Figure 6 shows the same images as the

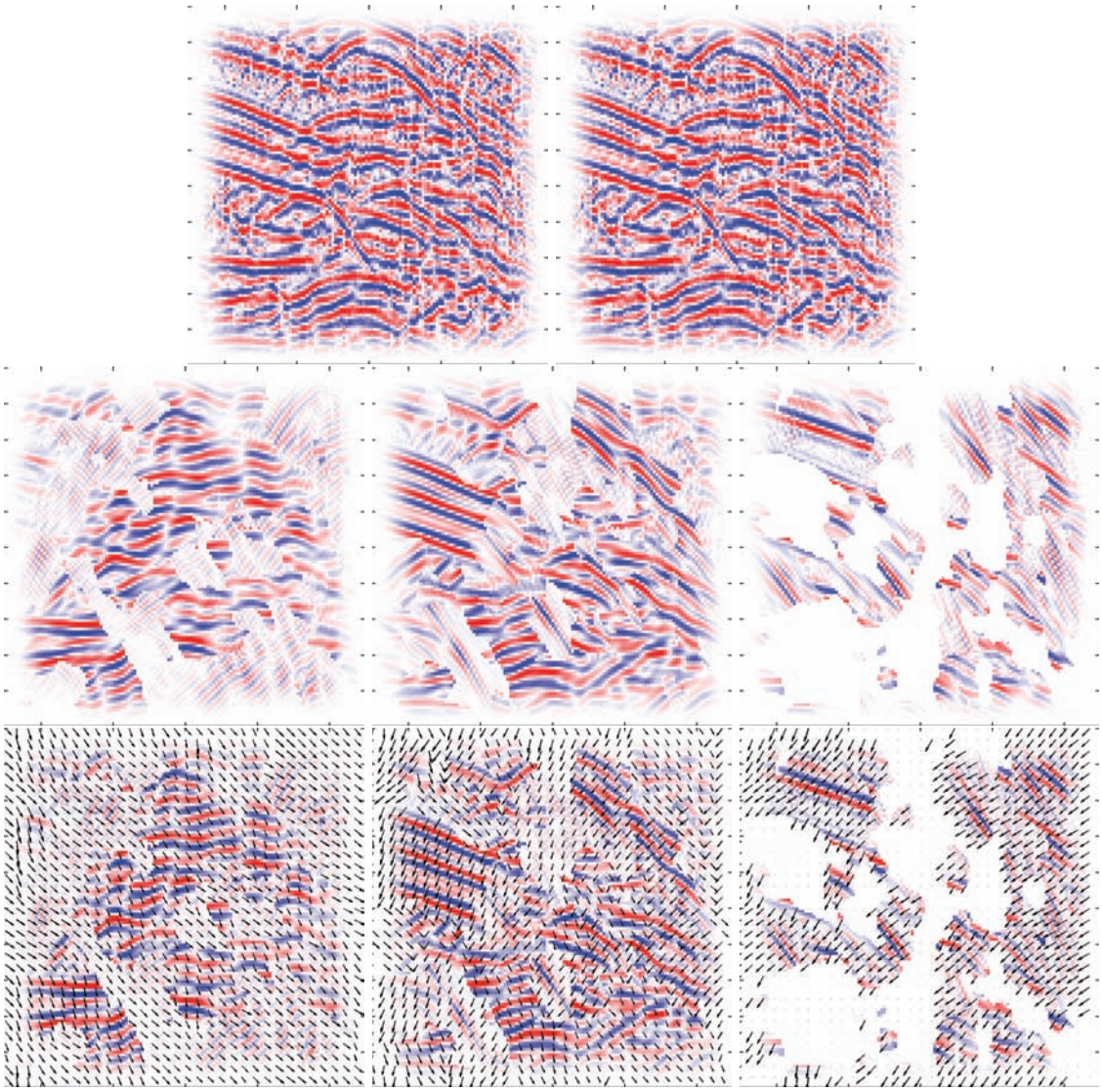

FIG. 6. *Processing results for a slice through the three dimensional data set shown in Figure 6. The top left panel shows the original data slice, and the top right panel show the sum of the three extracted components* ($\mathcal{G}_{\xi_1} f + \mathcal{G}_{\xi_2} f + \mathcal{G}_{\xi_3} f$. *All images are displayed with the same (thresholded) color scheme. The three middle panels show the extracted components* $\mathcal{G}_{\xi_1} f$, $\mathcal{G}_{\xi_2} f$ *and* $\mathcal{G}_{\xi_3} f$, *and the three bottom panels show the same images overlayed with quiver plots of the extracted directions (projected onto the viewing plane).*

middle panels, but with corresponding quiver plots overlayed.

7. Conclusions. By using the one way wave equation data can be extended so that it is possible to resolve intersecting oscillations from the eigenvalue decomposition of the structure tensors in the extended space–time domain. The eigenvectors corresponding to small eigenvalues can be used, in combination with the special structure introduced by the one way wave equation extension, to recover the intersecting oscillations. This method scales similarly in computational time as methods using the standard structure tensor (i.e., linearly with the number of samples). Once directionality estimations are obtained, it is possible to use a version of the one way wave equation where spatial points are deformed according predictions from the directionality estimations, in order to filter out the desired directions.

REFERENCES

[1] S. Arseneau and J. Cooperstock, *An improved representation of junctions through asymmetric tensor diffusion*, Advances in Visual Computing, (2006), pp. 363–372.

[2] G. Beylkin, *On the fast Fourier transform of functions with singularities*, Appl. Comput. Harmon. Anal., 2 (1995), pp. 363–381.

[3] J. Bigun and G.H. Granlund, *Optimal orientation detection of linear symmetry*, in First International Conference on Computer Vision, ICCV (London), 1987, pp. 433–438.

[4] David Cox, John Little, and Donal O'Shea, *Ideals, varieties, and algorithms*, Undergraduate Texts in Mathematics, Springer, New York, third ed., 2007. An introduction to computational algebraic geometry and commutative algebra.

[5] A. Dutt and V. Rokhlin, *Fast Fourier transforms for nonequispaced data*, SIAM J. Sci. Comput., 14 (1993), pp. 1368–1393.

[6] W. Förstner, *A framework for low level feature extraction*, Computer Vision – ECCV'94, (1994), pp. 383–394.

[7] W. Förstner and E. Gülch, *A fast operator for detection and precise location of distinct points, corners and centres of circular features*, in Proc. ISPRS intercommission conference on fast processing of photogrammetric data, 1987, pp. 281–305.

[8] I. Galić, J. Weickert, M. Welk, A. Bruhn, A. Belyaev, and H.P. Seidel, *Towards pde-based image compression*, Variational, Geometric, and Level Set Methods in Computer Vision, (2005), pp. 37–48.

[9] C. Harris and M. Stephens, *A combined corner and edge detector*, in Alvey vision conference, vol. 15, Manchester, UK, 1988, p. 50.

[10] FL Hitchcock, *Multiple invariants and generalized rank of a p-way matrix or tensor*, J. Math. Phys, 7 (1927), pp. 39–79.

[11] Guðbjörn F. Jónsson and Stephen A. Vavasis, *Accurate solution of polynomial equations using Macaulay resultant matrices*, Math. Comp., 74 (2005), pp. 221–262.

[12] H. Knutsson, C.F. Westin, and M. Andersson, *Representing local structure using tensors ii*, Image Analysis, (2011), pp. 545–556.

[13] U. Köthe, *Edge and junction detection with an improved structure tensor*, Pattern Recognition, (2003), pp. 25–32.

[14] E. Özarslan and T.H. Mareci, *Generalized diffusion tensor imaging and analytical relationships between diffusion tensor imaging and high angular resolution diffusion imaging*, Magnetic Resonance in Medicine, 50 (2003), pp. 955–965.

[15] T. Schultz, J. Weickert, and H.P. Seidel, *A higher-order structure tensor*, Visualization and Processing of Tensor Fields, (2009), pp. 263–279.

[16] D. Tschumperlé and R. Deriche, *Diffusion tensor regularization with constraints preservation*, in Computer Vision and Pattern Recognition, 2001. CVPR 2001. Proceedings of the 2001 IEEE Computer Society Conference on, vol. 1, IEEE, 2001, pp. I–948.

[17] D. Tschumperle and R. Deriche, *Vector-valued image regularization with pdes: A common framework for different applications*, Pattern Analysis and Machine Intelligence, IEEE Transactions on, 27 (2005), pp. 506–517.

[18] J. Weickert, *Anisotropic diffusion in image processing*, vol. 1, Teubner Stuttgart, 1998.

[19] L. Zhang, L. Zhang, and D. Zhang, *A multi-scale bilateral structure tensor based corner detector*, Computer Vision–ACCV 2009, (2010), pp. 618–627.